JOURNAL OF CATALYSIS 79, 34–46 (1983)

Sintering of Alumina-Supported Nickel and Nickel Bimetallic Methanation Catalysts in H_2/H_2O Atmospheres

C. H. BARTHOLOMEW, R. B. PANNELL, AND R. W. FOWLER

BYU Catalysis Laboratory, Department of Chemical Engineering, Brigham Young University, Provo, Utah 84602

Received March 2, 1982; revised August 24, 1982

Sintering of α- and γ-alumina- and nickel aluminate-supported nickel in H_2 and H_2O/H_2 atmospheres and alumina-supported Ni–Rh and Ni–Ru in H_2 was studied at temperatures between 773 and 1023 K. Total catalyst surface areas and metal surface areas were measured as a function of sintering time by argon BET and H_2 chemisorption, respectively. Phase compositions of the support and metal were investigated by X ray, while transmission electron microscopy, X-ray line broadening, and H_2 chemisorption were used to monitor changes in metal crystallite growth during heat treatments. The results indicate that significant losses in metal surface area occur as a result of (i) support collapse and (ii) metal crystallite growth in all of the catalysts. Nickel is most thermally stable on $NiAl_2O_4$ and more thermally stable on γ-Al_2O_3 than on α-Al_2O_3 (below 1023 K). Rhodium and ruthenium additives enhance the thermal stability of nickel on alumina. Differential activity tests indicate that no significant changes in specific methanation activity occur for alumina-supported nickel catalysts as a result of sintering, although Ni–Rh and Ni–Ru catalysts produce a higher fraction of C_{2+} hydrocarbons after heat treatment.

INTRODUCTION

Thermal degradation of nickel catalysts is a problem in a number of high-temperature catalytic processes such as steam reforming and methanation of coal synthesis gas. Thermal deactivation of supported nickel may result from (i) sintering (i.e., loss of support and metal area), and (ii) phase transformations such as the formation of nickel aluminate.

There have been relatively few previous investigations of sintering of supported nickel (*1–8*). Only five of these were systematic investigations of sintering per se (*1, 5–8*) and only two of these studies (*1, 5*) reported sintering rates of Ni/Al_2O_3 in H_2 or H_2O/H_2 atmospheres; in the other studies (*2–4*) thermal treatments were employed mainly to change the metal crystallite size in order to determine effects of crystallite size on adsorption or rates of reaction. None of the previously reported investigations of supported nickel considered effects of support properties or metal/metal oxide promoters on the rates of sintering of Ni/Al_2O_3 [although preliminary data on two Al_2O_3 supports were reported in our earlier study (*5*)]. Moreover, none of the previous investigations provided definitive evidence as to the nature of sintering of Ni/Al_2O_3 in H_2/H_2O atmospheres, i.e., whether it is a result of nickel crystallite growth or collapse of the support or a combination of both, nor did they provide data on the effects of sintering on catalytic activity.

The present study was undertaken to determine (i) the nature of the loss of nickel surface area during sintering of Ni/Al_2O_3, (ii) the effects of support pretreatment and metal/metal oxide promoters on sintering rates of Ni/Al_2O_3, and (iii) effects of sintering on the specific methanation activity/selectivity properties of nickel. To accomplish these objectives, the effects of high temperatures on support and metal crystallite properties (surface area, pore size, crystallite size, etc.) of alumina-supported

0021-9517/83/010034-13$03.00/0

Ni, Ni–Ru, and Ni–Rh in H_2 and H_2O/H_2 atmospheres were examined as a function of time. The effects of calcining the support at high temperature prior to catalyst preparation were also examined.

EXPERIMENTAL

Materials

Analytically pure $Ni(NO_3)_2 \cdot 6H_2O$ (Baker Analyzed) and Kaiser SAS 5 × 8-mesh γ-alumina (initially 301 m^2/g) were used to prepare two 15 wt% nickel-on-alumina catalysts (A and B) by simple impregnation (*9, 10*). Catalyst A was prepared on Al_2O_3 which had been previously calcined in air at 1173 K, whereas Catalyst B was prepared on γ-Al_2O_3 calcined at only 923 K. Also prepared by impregnation of $NiAl_2O_4$ was 15% $Ni/NiAl_2O_4$. The nickel aluminate support was made by stepwise impregnation of a Catapal (Conoco) alumina with nickel nitrate, drying at 373 K for several hours, and after the third and fifth (final impregnation), heating to 523 K for 2 hr and 925 K for 4 hr in air; the final support contained 15 wt% nickel. The Ni–Ru and Ni–Rh catalysts were prepared on the Kaiser alumina calcined at 1173 K. Chloride salts of Ru and Rh, combined with nickel nitrate in mild acid solution to prevent hydrolysis, were used to impregnate the alumina pellets. Each catalyst was reduced in purified, flowing hydrogen at 723 K following a previously reported temperature program (*9, 10*).

Hydrogen (99.9%) was purified by passing it through both a palladium Deoxo purifier (Engelhard) and dehydrated molecular sieve. For the 3% H_2O/H_2 runs, the hydrogen was bubbled through a flask containing distilled water.

Apparatus and Procedure

Initial and final overall surface areas were determined by BET measurements. Hydrogen adsorption uptakes were determined as a function of time intermittently during sintering from static adsorption measurements at 298 K assuming one hydrogen atom adsorbed on each surface metal atom (*11, 12*). BET, H_2 uptake, and activity/selectivity measurements were carried out using the same quartz cell as used in sintering measurements, such that the sample was not exposed to air.

Sintering studies were carried out in an all-quartz laboratory reactor equipped with preheater coils and an in-the-bed thermocouple for accurate catalyst bed temperature measurements (*10*). Hydrogen was passed over the catalyst at 903, 923, or 1023 K (or at 773, 848, 903, or 1023 K in the runs using 3% water/H_2) for a period of 13–200 hr. A tubular quartz furnace connected to a temperature-programmed controller was used to maintain constant temperature throughout each experiment.

Catalyst activities were measured at 498, 523, and 548 K in a reactant stream of 95% N_2, 4% H_2, and 1% CO before and after thermal treatments. Reactant and product gases were analyzed by gas chromatography using a thermal conductivity detector. Samples were ground to a 100- to 150-mesh powder and run at high space velocities in order to minimize heat/mass transport effects and pore diffusional influences on rate.

Powdered catalyst samples were submitted for X-ray diffraction patterns and for electron microscope analysis to determine particle size independent of chemisorption measurements.

Transmission electron micrographs were obtained for both fresh and sintered catalyst samples. Reduced, passivated samples were crushed in a mortar and pestle, placed in *n*-butanol, and ground to a fine powder. The resulting mixture was ultrasonicated for 5 min to evenly distribute the fine particles. A drop of this mixture was placed on a Formvar-coated copper grid, the *n*-butanol allowed to evaporate, and the grid coated with a fine layer of carbon to permit sample stability in the electron beam. The prepared grids were then examined using a Hitachi

HU-11E transmission electron microscope. Several photographs of each sample were used in obtaining a particle size distribution.

X-ray diffraction scans were obtained using a Phillips diffractometer equipped with a graphite monochromater. The interplanar spacings for the various diffractogram peaks were calculated using the Bragg equation with $\lambda = 0.15405$ nm (Cu $K\alpha$ radiation) and $n = 1$. Metal particle sizes were estimated from X-ray line broadening using the Scherrer equation according to the method of Klug and Alexander (*13*).

RESULTS

BET and metal surface area data (in the form of H_2 uptakes at 298 K) for alumina-supported Ni, Ni–Ru, and Ni–Rh catalysts sintered at 898 or 903, 923, and 1023 K in pure hydrogen and for Ni/Al_2O_3 at 773, 848, 903, and 1023 K in 3% water in hydrogen are shown in Table 1. Hydrogen uptake versus time data are plotted in Figs. 1 and 2. Values of dispersion (percentage metal exposed to the surface) calculated from hydrogen chemisorption uptakes at 298 K are also listed for each of the samples in Table 1.

Data in Table 1 for Catalyst A (support calcined at 1173 K) show reductions in overall surface area of 20 and 30% and in hydrogen chemisorption of 27 and 44% after exposure to a hydrogen atmosphere for

TABLE 1

Sintering Data for Alumina-Supported Nickel

Catalyst	Atmosphere	Time (hr)	Temperature (K)	H_2 uptake (μmole/g cat)	BET area (m^2/g)	Percentage dispersion[a]
15% Ni/Al_2O_3,[b]	(Fresh)	0	—	236	98.3	18.4
Catalyst A	H_2	65	903	182		14.2
	H_2	130	903	173	78.4	13.5
15% Ni/Al_2O_3,[b]	(Fresh)	0	—	218	98.3	17.0
Catalyst A	H_2	36	1023	125		9.7
	H_2	72	1023	122	68.8	9.5
15% Ni/Al_2O_3,[c]	(Fresh)	0	—	227	148	17.7
Catalyst B	H_2	70	923	202		15.8
	H_2	140	923	170		13.2
	H_2	210	923	182	117	14.2
15% Ni/Al_2O_3,[c]	(Fresh)	0	—	225	148	17.5
Catalyst B	H_2	51	1023	154		12.0
	H_2	100	1023	145	110	11.3
15% Ni/Al_2O_3,[b]	(Fresh)	0	—	235	98.3	18.3
Catalyst A	3% H_2O/H_2	5	773	253		19.7
	3% H_2O/H_2	30	773	233		18.2
	3% H_2O/H_2	72	773	240		18.7
	3% H_2O/H_2	66	848	198		15.4
	3% H_2O/H_2	137	848	197	73.8	15.4
15% Ni/Al_2O_3,[b]	(Fresh)	0	—	225	98	17.6
Catalyst A	3% H_2O/H_2	4	898	212		16.5
	3% H_2O/H_2	9	898	194		15.1
	3% H_2O/H_2	13	898	159		12.4
15% Ni/Al_2O_3,[b]	(Fresh)	0	—	225	98	17.6
Catalyst A	3% H_2O/H_2	6	1023	114		8.9
	3% H_2O/H_2	13	1023	121	58.2	9.4

TABLE 1—*Continued*

Catalyst	Atmosphere	Time (hr)	Temperature (K)	H_2 uptake (μmole/g cat)	BET area (m^2/g)	Percentage dispersion[a]
15% $Ni/NiAl_2O_4$	(Fresh)	0	—	163	82.4	
	H_2	4	1023	205		
	H_2	9	1023	168		
	H_2	15	1023	174		
	H_2	22	1023	181		
	H_2	30	1023	200		
	H_2	40	1023	159		
	H_2	50	1023	189	57.0	
16.7% Ni, 3.3% Ru/Al_2O_3[b]	(Fresh)	0	—	181	85.6	10.6
	H_2	6	898	161		9.4
	H_2	10	898	156		9.1
	H_2	14	898	158	74.4	9.2
16.7% Ni, 3.3% Ru/Al_2O_3[b]	(Fresh)	0	—	179	85.6	10.5
	H_2	6	1023	190		11.1
	H_2	12	1023	137		8.0
	H_2	18	1023	133	72.9	7.8
	H_2	24	1023	139		8.1
16.7% Ni, 3.3% Rh/Al_2O_3[b]	(Fresh)	0	—	138	86.	8.1
	H_2	4	898	118		6.9
	H_2	8	898	122		7.1
	H_2	12	898	110		6.4
	H_2	16	898	113	74.4	6.6
16.7% Ni, 3.3% Rh/Al_2O_3[b]	(Fresh)	0	—	138		8.1
	H_2	3.3	1023	117		6.8
	H_2	6.6	1023	153		9.0
	H_2	9.9	1023	113		6.6
	H_2	14	1023	118		6.9
	H_2	18	1023	106		6.2
	H_2	26	1023	109		6.4

[a] $\% D = X(1.17)/W$, where X = H_2 uptake and W = wt% metal; based on site density for nickel (average of three lowest index planes) of 6.77×10^{-2} nm^2/atom. Effects of Rh and Ru additives on site density are assumed to be small.

[b] Catalyst prepared on alumina calcined at 1173 K prior to impregnation with $Ni(NO_3)_2 \cdot 6H_2O$.

[c] Catalyst prepared on alumina calcined at 923 K prior to impregnation with $Ni(NO_3)_2 \cdot 6H_2O$.

130 hr at 903 K and for 72 hr at 1023 K, respectively. Hence, the loss of metal surface area was greater than the loss of total area at 1023 K, while at 903 K the metal area decrease was approximately equal to the total area decrease.

Similar results were obtained for Catalyst B; however, the losses in both BET and hydrogen chemisorption were either less than or equal to those for Catalyst A. That is, the decreases in hydrogen uptake for Catalyst B were 20 and 35% and the decreases in BET area were 21 and 25% at 923 and 1023 K, respectively. Again, at 1023 K the percentage loss in hydrogen uptake was significantly higher than the loss of BET area.

The metal dispersion versus time data for the two nickel catalysts were fitted to a rate equation of the form $-dD/dt = kD^n$ (where D is dispersion and n the order of sintering) to determine sintering rate constants and activation energies listed in Table 2. Although data for Catalyst A were best fitted

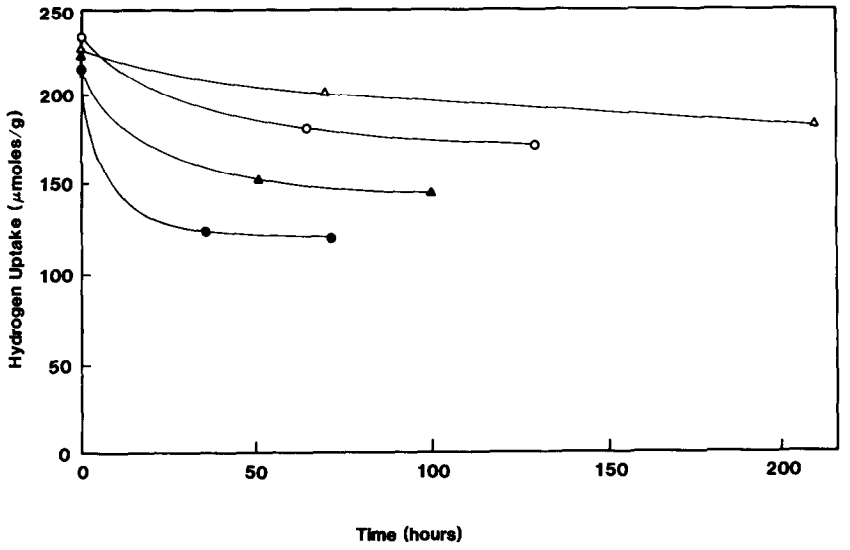

FIG. 1. Nickel metal surface area loss during sintering; effect of temperature and support pretreatment. △, 15% Ni/Al_2O_3 (923 K support; Catalyst B) at 923 K; ▲, 15% Ni/Al_2O_3 (923 K support; Catalyst B) at 1023 K; ○, 15% Ni/Al_2O_3 (1173 K support; Catalyst A) at 903 K; ●, 15% Ni/Al_2O_3 (1173 K support; Catalyst A) at 1023 K.

to $n = 10$ while those for Catalyst B were best fitted to $n = 7$, the correlation coefficients were not sensitive to n in the range $n = 7$–10. Thus to be consistent, data reported in Table 2 are based on $n = 7$. The significantly larger rate constants for Catalyst A indicate that it sinters more rapidly than Catalyst B in the temperature range 900–1023 K. However, the smaller activation energy calculated for Catalyst A indicates that at a sufficiently high temperature (above 1023 K) Catalyst B will sinter more rapidly.

The H_2 uptake and dispersion versus

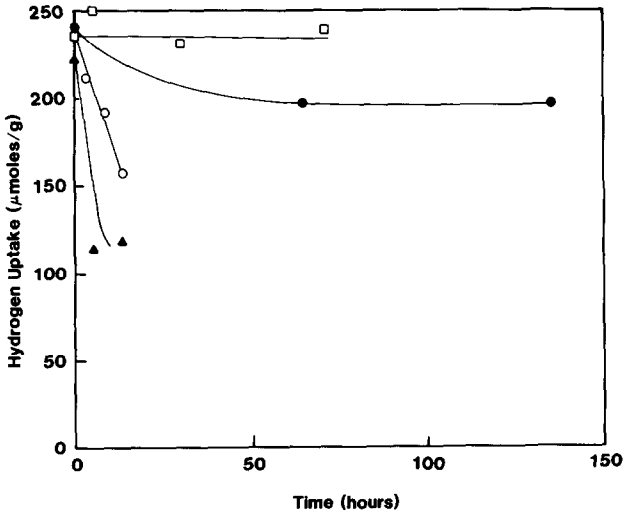

FIG. 2. Effect of 3% H_2O on sintering of 15% Ni/Al_2O_3 (Catalyst A–1173 K support) at: □, 773 K; ●, 848 K; ○, 898 K; ▲, 1023 K.

TABLE 2

Sintering Rate Constants and Activation Energies for Ni/Al_2O_3 Sintering[a,b]

Catalyst	Temp. (K)	k (hr^{-1})[b]	E_{act} (kJ/mole)[b]
A	923	400	165
A	1023	3290	
B	923	78.2	197
B	1023	964	

[a] Calculated for temperature range 900–1023 K.
[b] Calculated from the rate equation $-dD/dt = kD^n$, where $k = A \exp[-E/RT]$; D = dispersion and $n = 7$.

time data for $Ni/NiAl_2O_4$ in Table 1 show that within experimental error (±10%) no significant loss in metal surface area occurred during 50 hr of sintering at 1023 K in H_2. However, a 31% loss in BET surface area was observed. Moreover, in an independent experiment in which the $NiAl_2O_4$ support was sintered 50 hr in H_2 at 1123 K an increase in H_2 uptake from 0 to 80.7 μmole/g was observed. In addition, X-ray diffraction data for fresh and sintered samples of $Ni/NiAl_2O_4$ provided evidence of an increase in average nickel crystallite diameter during the sintering process. Accordingly, the data show that the loss of nickel surface area in the sintering process was compensated for by the creation of new nickel crystallites via reduction of the support.

Data in Table 1 and Fig. 2 show the effects on H_2 uptake and BET surface area of sintering 15% Ni/Al_2O_3 (A) in 3% H_2O/H_2 at four different temperatures. The decreases in BET and metal surface areas over a period of 72 hr at 773 K were negligible. However, after 137 hr at 848 K decreases in BET and hydrogen chemisorption of 25 and 16%, respectively, were observed. Rates of Ni/Al_2O_3 sintering at 923 and 1023 K in 3% H_2O were significantly higher than those in pure H_2. For example, only 13 hr at 1023 K in 3% H_2O was required for the same change in nickel area as occurred after 72 hr in pure H_2, and the loss of support area was 41% in the H_2O-containing atmosphere after 13 hr compared to 30% in pure H_2 after 72 hr. At 1023 K, the percentage decreases in H_2 uptake and BET surface area were nearly the same (49 and 42%, respectively).

Hydrogen uptakes are plotted as a function of time in Fig. 3 for samples of Ni–Rh

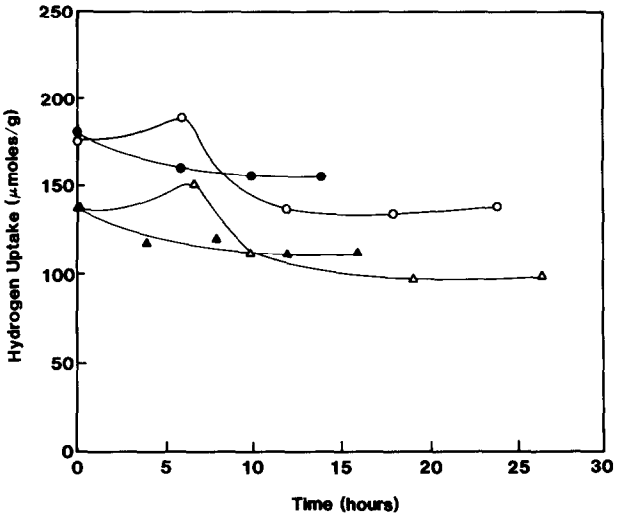

FIG. 3. Metal surface area loss during sintering for Ni–Rh and Ni–Ru bimetallics. ●, 16.6% Ni–3.4% Ru/Al_2O_3 at 898 K; ○, 16.6% Ni–3.4% Ru/Al_2O_3 at 1023 K; ▲, 16.6% Ni–3.4% Rh/Al_2O_3 at 898 K; △, 16.6% Ni–3.4% Rh/Al_2O_3 at 1023 K.

and Ni–Ru. At 898 K both Ni–Rh and Ni–Ru exhibit exponential-like decays in H_2 uptake. However, at 1023 K both show maxima in H_2 uptake after about 8 hr after which an exponential decay is observed. Data in Table 1 for the nickel bimetallic catalysts show that their percentage losses in support area were essentially equal to those of the nickel catalysts at both temperatures. However, the percentage losses in metal surface area for Ni–Rh and Ni–Ru were about a factor of 2 less than those for 15% Ni/Al_2O_3 at both temperatures.

Metal crystallite diameters estimated from electron microscopy, X-ray diffraction line broadening, and H_2 chemisorption measurements are listed in Table 3. The particle size distributions for fresh and sintered 15% Ni/Al_2O_3 are shown in Fig. 4. X-ray diffraction peaks for samples of fresh Ni/Al_2O_3 were too diffuse or masked by interfering Al_2O_3 peaks to enable crystallite diameters to be estimated. Crystallite diameters estimated from the (200) X-ray diffraction lines for nickel sintered 72 hr at 1023 K in H_2 and 13 hr at 1023 K in 3% H_2O/H_2 of 4.6 and 4.1 nm, respectively, were two to three times lower than those estimated by other techniques. However, surface mean particle diameters from transmission electron microscopy (TEM) of 4.6, 10.8, and 12.0 nm for fresh, 1023 K sintered, and 1023 K sintered in 3% H_2O/H_2 samples of Ni/Al_2O_3, respectively, were in good agreement with those determined by H_2 adsorption.

TABLE 3

Estimates of Metal Crystallite Diameter from Electron Microscopy, X-Ray Line Broadening, and H_2 Chemisorption at 298 K

Catalyst	Crystallite diameter (nm)		
	TEM[a]	X ray[b]	H_2 chemisorption[c]
Ni/Al_2O_3 (A)			
Fresh	3.7, 4.6	—	5.7
1023 K	9.3, 10.8	4.6[d]	10.2
1023 K c 3% H_2O	10, 12	4.1[d]	10.2
$Ni–Ru/Al_2O_3$			
Fresh	10.7, 16.0	7.6,[e] 5.6[d]	8.3
1023 K	19.2, 25	7.7,[e] 5.8[d]	10.8
$Ni–Rh/Al_2O_3$			
Fresh	17.7, 22	10,[e] 7.2[d]	10.8
1023 K	18.4, 27	13,[e] 8.3[d]	13.7

[a] Transmission electron microscopy data include area, and volume mean diameters, respectively.

[b] From line broadening using Scherrer equation.

[c] Based on total H_2 volumetric uptake at 298 K assuming spherical crystallites of the same diameter and complete reduction to the metal.

[d] (200) plane.

[e] (111) plane—partially masked by Al_2O_3 peaks.

Estimates of crystallite diameter from TEM for fresh Ni–Ru and Ni–Rh catalysts were significantly larger than those calculated from either X ray or H_2 adsorption; the crystallite diameters estimated from the (111) X-ray plane were generally in good agreement with the estimates from H_2 adsorption. In the case of Ni–Ru, estimates of the percentage particle size growth due to sintering varied greatly for the three different techniques, i.e., 56, 1, and 30% for TEM, X ray, and H_2 adsorption, respectively. On the other hand, the estimates of percentage particle size growth for Ni–Rh from TEM, X ray, and H_2 adsorption of 22, 30, and 27% were in good agreement.

The chemical phase composition of the alumina support was determined from X-ray scans of fresh, calcined or sintered samples of the support and catalysts. Calcination of the γ-Al_2O_3 at 923 K (2 hr) caused only minor modifications in the support structure; that is, γ-Al_2O_3 was the major crystalline phase even though approximately 30–40% pore volume was lost and the BET surface area decreased from about 300 to 150 m^2/g. Calcination at 1173 K, however, resulted in a substantial conversion of γ-Al_2O_3 to α- and δ-Al_2O_3. In the Ni(A), Ni–Rh, and Ni–Ru catalysts (fresh or sintered), the dominant alumina phases present were α- and δ-alumina; γ-Al_2O_3 was the dominant support phase in Ni(B).

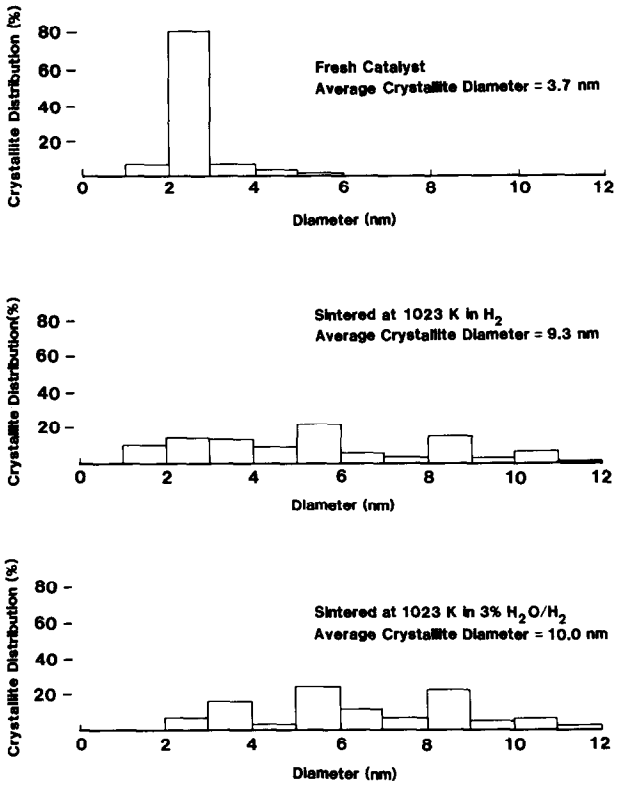

FIG. 4. Particle size distributions (surface averaged values) for fresh and sintered 15% Ni/Al_2O_3 (support pretreated at 1173 K) from transmission electron microscopy.

From extended BET measurements it was possible to determine pore volumes and average pore radii for fresh and sintered support and catalyst samples (see Table 4). As the calcination temperature was increased from 673 to 1173 K the pore volume of the support decreased from 0.43 to 0.20 ml/g. Exposing the support previously calcined at 1173 K in a reducing atmosphere caused a further decrease in pore volume from 0.20 to 0.15 ml/g after 130 hr at 923 K and to 0.13 ml/g after 120 hr at 1023 K in H_2. Ni, Ni–Rh, and Ni–Ru catalysts exhibited similar changes in volume for similar time and temperature treatments with the exception of the Ni/Al_2O_3 treated in 3% H_2O/H_2. The pore volume of this catalyst was reduced to one-half its original value (0.20 to 0.10 ml/g) in only 14 hr, while the support treated at 1023 K for 120 hr in H_2 lost only one-third its pore volume. Increases in the average pore radius of 15–30% for alumina and alumina-supported nickel and nickel bimetallic catalysts as a result of high-temperature treatments in air or H_2 were also generally observed.

Methanation activity data determined at 498 K and 120 kPa are listed in Table 5 for fresh and sintered samples of alumina-supported Ni, Ni–Rh, and Ni–Ru. Specific activities (i.e., turnover numbers) and product yields were apparently unaffected by the high-temperature treatments in H_2 within the experimental precision of the measurements (estimated to be ±15%). For example, at 498 K the fresh nickel catalyst had a turnover number of 2.6×10^{-3} s^{-1} and a methane selectivity of 0.77 (selectivity defined as the fraction of CO converted to a given product) compared to a turnover number of 3.0×10^{-3} s^{-1} and a methane selectivity of 0.83 after sintering at 1023 K.

TABLE 4

Pore Volume and Average Pore Radius from Physical Adsorption Measurements

Sample	Pore volume (ml/g)	Average radius (nm)	BET surface area (m^2/g)
Support 673 K, 2 hr, air	0.428	5.8	198
Support 873 K, 2 hr, air	0.321	7.0	150
Support 1173 K, 24 hr, air	0.200		79
Support 1173 K, 24 hr, air, then 130 hr at 923 K in H_2	0.145	7.5	94
Support 1173 K, 24 hr, air, then 120 hr at 1023 K in H_2	0.134	8.7	88
Ni/Al_2O_3 (Catalyst A)			
Fresh	0.204	7.0	86
1023 K in H_2	0.134	8.4	68
1023 K in 3% H_2O	0.103	7.5	58
$Ni–Ru/Al_2O_3$			
Fresh	0.163	5.6	86
898 K, 14 hr in H_2	0.146	8.2	74
$Ni–Rh/Al_2O_3$			
898 K, 16 hr in H_2	0.135	8.4	74

There were, however, significant increases in the selectivity for C_{2+} hydrocarbons observed for the Ni–Ru and Ni–Rh catalysts after sintering at 1023 K.

DISCUSSION

Sintering of Ni/Al_2O_3 in Hydrogen

One of the important questions regarding the sintering of nickel on alumina not adequately addressed in previous studies was whether loss of nickel surface area is a result of crystallite growth, support collapse, or a combination of both. The combination of H_2 adsorption, X-ray, TEM, and pore size data from this study provides new insights in this regard.

The data in Table 1 suggest that the loss of metal surface area is highly correlated with the loss of BET or support areas at sintering temperatures below 923 K. Since the percentage loss of support area and that of metal area are of the same magnitude (in many cases nearly equal), the loss of support area may be a major cause of the loss of metal area. Williams *et al.* (*1*) concluded

TABLE 5

Effects of Sintering on Methanation Activities of Nickel and Nickel Bimetallics at 498 K and 120 kPa

Catalyst/temperature of treatment	H_2 uptake (μmole/g)	Percentage CO conversion	Percentage selectivity[a]			Methane turnover No.[b] ($\times 10^3$ (s^{-1}))	Activation energy[c] (kJ/mole)
			CH_4	CO_2	C_{2+}		
Ni/Al_2O_3 (A)							
Fresh	235	8.5	0.77	0.01	0.22	2.6	91
903 K	173	8.6	0.81	0.00	0.19	3.0	84
1023 K	133	4.9	0.83	0.00	0.17	2.3	86
$Ni–Ru/Al_2O_3$							
Fresh	179	2.1	0.84	0.03	0.13	1.2	102
1023 K	139	3.2	0.55	0.01	0.44	1.4	98
$Ni–Rh/Al_2O_3$							
Fresh	138	5.1	0.75	0.04	0.21	0.84	79
1023 K	109	3.0	0.45	0.09	0.46	1.7	96

[a] Selectivity is the fraction of converted CO appearing as a given product.

[b] Methane turnover number (frequency) is the number of methane molecules produced per catalytic site (based on H_2 uptake at 298 K) per second.

[c] Determined over the temperature range 498 to 548 K for methanation formation.

that in Ni/Al_2O_3 the nickel crystallites are not buried but rather the loss of nickel surface area occurs due to loss of fine pore structure and/or conversion of γ-Al_2O_3 to α-Al_2O_3. However, pore size distribution data from this study are not consistent with a loss of fine structure since the average pore radius does not change significantly even though pore volume does. These changes are more indicative of a reduction in pore length at constant radius. This would imply that some nickel crystallites are buried or at least blocked off. Moreover, the X-ray data from this study show that in Ni/γ-Al_2O_3 catalysts for which the support was pretreated and which were sintered at 923 K, the major support phase remains as γ-Al_2O_3.

In addition to the loss of nickel area due to support collapse, the data of companion studies (*14, 15*) provide evidence that increases in Ni metal crystallite size occur during sintering of Ni/γ-Al_2O_3 at 923 K. Hence the loss of nickel surface area at 923 K in Ni/γ-Al_2O_3 catalysts is due to a combination of crystallite growth and support collapse. Desai and Richardson (*7*) reached similar conclusions in their study of Ni/SiO_2 catalysts thermally treated at 873 to 973 K.

The data for both nickel catalysts A and B show that metal area loss increases relative to support area loss as temperature is increased from 903 or 923 to 1023 K suggesting that metal sintering becomes more important than support collapse at temperatures above 903–923 K. Indeed, the data in Table 3 show that very significant increases (~100–200%) in nickel crystallite size occur in Ni/Al_2O_3 after sintering at 1023 K in H_2. In addition the X-ray data show that the support changes from predominantly γ-Al_2O_3 to α- and δ-Al_2O_3 forms after treatment at 1123 K. Thus, losses in support area and changes in support structure undoubtedly also contribute to the loss of nickel surface area at the higher sintering temperatures such as 1023 K. However, in view of the close agreement between crystallite size estimates from TEM and H_2 adsorption for Ni/Al_2O_3, growth of metal crystallites is apparently the predominant effect.

The fact that the sintering rate data for Ni/Al_2O_3 were best fitted to the rate equation $-dD/dt = kD^n$, where $n = 7-10$, also suggests that the sintering process for nickel on alumina is typical of metal sintering where values of n range from 2 to 12 (*15, 16*).

Effects of 3% Water

Data from Table 1 and Fig. 2 show that treatment of Ni/Al_2O_3 in 3% H_2O/H_2 for 70 hr at 773 K causes negligible sintering. Williams *et al.* (*1*) reported very significant losses of surface area during the first 100 hr for Ni/Al_2O_3 treated at 673 and 773 K in an atmosphere of $H_2O/H_2 = 9$. Apparently low concentrations of water (e.g., 3% H_2O/H_2 as in the study) do not have the same effect on Ni/Al_2O_3 at these temperatures. At 923 and 1023 K rates of metal and support sintering in 3% water are greatly enhanced over the rates in the absence of water. The percentage loss in metal area of 46% is only slightly larger than the loss in support area of 41% at 1023 K. Thus, the collapse of the support plays a more important role in loss of nickel surface area when water vapor is present. Nevertheless, the growth of nickel crystallites at 1023 K is significant (see Table 3). Besides crystallite growth and support collapse, loss of nickel surface area might occur in Ni/Al_2O_3 at high temperatures in the presence of water as a result of NiO or $NiAl_2O_4$ formation. Nevertheless, the X-ray data from this study showed no evidence of $NiAl_2O_4$ being formed after exposure to 3% H_2O/H_2. Moreover, H_2 uptakes at 298 K and O_2 titration data at 723 K indicated that NiO was apparently not formed after treatment at 1023 K in 3% H_2O/H_2.

Effects of Alumina Phase Composition on Sintering

Contrary to initial expectations the effect of increasing the temperature for calcination of the support prior to preparation was

to lower the resistance of the catalyst to sintering in reducing atmospheres. The higher sintering rates for Catalyst A relative to B (Table 2 and Fig. 1) support this conclusion. This result is surprising since one might expect that presintering the support at 1173 K in an oxidizing atmosphere would decrease its tendency to lose area at lower temperatures in either oxidizing or reducing atmospheres. The fact that the γ-Al_2O_3 support was converted to α and δ forms at 1123 K is not surprising since this phase transition is well known (*17*). What is surprising is that the losses in BET surface area at 1023 K were about the same for Ni(A) and Ni(B), since one might expect α- and δ-Al_2O_3 to be more stable than γ-Al_2O_3. Apparently the high-temperature formation of γ- and δ-Al_2O_3 resulted in a support more prone to thermal degradation in hydrogen atmosphere than γ-Al_2O_3. In addition, the greater tendency of Ni(A) to lose H_2 uptake suggests that migration and growth of metal crystallites occurred more readily on the support treated at 1173 K. This behavior is consistent with the observation (*18*) that such high-temperature treatment of the support causes loss of hydroxyl groups thereby decreasing the interaction of support and metal. Nevertheless, the lower activation energy for sintering of Catalyst A(Ni/α-Al_2O_3) relative to B(Ni/γ-Al_2O_3) indicates that at very high sintering temperatures (i.e., significantly above 1023 K), nickel will be more stable on α-Al_2O_3.

It is interesting to compare the activation energies for sintering of nickel on α- and γ-alumina forms from Table 2 of 165 and 197 kJ/mole with a value of 399 kJ/mole reported for sintering of nickel on silica in H_2 (*15*). The significantly lower activation energies for Ni/Al_2O_3 suggest that nickel may be more thermally stable when supported on either α- or γ-Al_2O_3 compared to SiO_2. This conclusion is supported by a recent companion study of Ni/SiO_2 and Ni/γ-Al_2O_3 in this laboratory (*15*).

The fact that the Ni/$NiAl_2O_4$ catalyst exhibited essentially no measurable decrease in H_2 adsorption capacity after sintering for 50 hr at 1023 K indicates that this particular catalyst possesses remarkable thermal stability at high temperatures, making it an ideal candidate for high-temperature applications, e.g., high-temperature methanation. The origin of this stability can be attributed to the very stable perovskite structure of $NiAl_2O_4$ and its ability to produce new hydrogen adsorption sites via reduction at very high temperatures which replace those lost through crystallite growth and support collapse. The unusual thermal stability of nickel on $NiAl_2O_4$ explains why calcination of high-loading commercial nickel catalysts at 700–800 K prior to reduction is common practice.

Sintering of Ni Bimetallics/Al_2O_3 in Hydrogen

Data in Table 1 and Figs. 1 and 3 for Ni, Ni–Rh, and Ni–Ru catalysts at 1023 K show that the fractional loss of metal surface area for Ni/Al_2O_3 after about 25 hr in H_2 is approximately twice that of Ni–Rh and Ni–Ru. Thus, rhodium and ruthenium apparently promote the thermal stability of nickel on alumina. The increase in metal surface area observed for Ni–Rh and Ni–Ru catalysts during the first 8 hr exposure to H_2 at 1023 K may result from reduction of metallic oxides to metal phases and possibly metal alloy phases. While the X-ray data for Ni–Rh and Ni–Ru were consistent with this possibility they did not provide conclusive evidence of alloy formation. The lower initial dispersions of Ni–Rh and Ni–Ru catalysts relative to the Ni catalysts are undoubtedly due in part to the slightly acidic pH during the impregnation of the bimetallics which resulted in eggshell distributions of the active catalytic phase and thus higher localized metal loadings on the alumina pellet.

Effects of Sintering in H_2 on Methanation Activity

Activity and selectivities for catalysts before and after high-temperature treatments

were generally the same within experimental accuracy. This leads to the conclusion that the active sites on the sintered catalysts are essentially the same as those on the unsintered samples. This result suggests that methanation is a facile rather than a demanding reaction (*19*) since X-ray, TEM, and H_2 chemisorption measurements show significant changes in the average metal crystallite diameter. This conclusion finds support from two other recent studies (*20, 21*). Bartholomew *et al.* (*20*) found that the specific methanation activity of Ni on Al_2O_3 was essentially the same as that on polycrystalline Ni and independent of crystallite size in moderate- to high-loading Ni catalysts (>5% Ni) in which metal–support interactions were minimal. Kelley *et al.* (*21*) found the specific methanation activity to be independent of the specific crystallographic plane, i.e., the same for Ni (100) and Ni (110). In the case of Ni–Ru, the large increase in C_{2+} at 498 K may indicate enrichment of the surface in Ru since Ru is more selective for production of C_{2+} hydrocarbons than Ni (*22*).

CONCLUSIONS

1. The loss of nickel surface area in Ni/γ-Al_2O_3 during high-temperature exposure to H_2 atmosphere is a result of two factors: (i) collapse of the support structure, and (ii) growth of metal crystallites accompanied by significant broadening of the crystallite size distribution. At 900–925 K, the loss of nickel area correlates highly with the loss of support area, suggesting that support collapse may be an important effect. At temperatures greater than 925 K the loss of metal area due to crystallite growth becomes a major factor.

2. Water vapor significantly accelerates the rate of sintering of Ni/Al_2O_3 in H_2 atmosphere at temperatures above about 800 K. The major effect of water appears to be the enhanced collapse of the support.

3. The chemical and physical structure of the support has a very significant influence on the rate at which supported nickel sinters. Nickel supported on γ-Al_2O_3 is significantly more thermally stable than nickel on α or δ forms. Both α- and γ-alumina supports contribute greater thermal stability to nickel than silica. However, nickel aluminate apparently provides the more thermally stable environment for nickel compared to α- and γ-Al_2O_3 supports because of its inherent chemical stability and because it can provide new nickel sites via high-temperature reduction of $NiAl_2O_4$.

4. Addition of Rh and Ru metal promoters significantly improves the stability of Ni/Al_2O_3 catalysts toward sintering.

5. Sintering in H_2 at high temperatures of Ni/Al_2O_3 and promoted Ni/Al_2O_3 catalysts has little influence on their methanation activity suggesting that this reaction is facile. Increases in the selectivity of Ni–Rh and Ni–Ru following sintering at 1023 K may result from changes in the surface composition of the bimetallic metal surfaces.

ACKNOWLEDGMENTS

We are indebted to Dr. Charles Pitt, University of Utah, for X-ray diffraction measurements and to Mark Jeffrey, Kevin Mayo, Donald Mustard, and Gordon Weatherbee for aid in experimental measurements. The authors gratefully acknowledge financial support from the National Science Foundation (ENG 75-00254), the Energy Research and Development Administration (Contract E(49-18)-1790), and the Union Oil Foundation.

REFERENCES

1. Williams, A., Butler, G. A., and Hammonds, J., *J. Catal.* **24,** 352 (1972).
2. Hughes, T. R., Houston, R., and Sieg, R. P., *Ind. Eng. Chem. Process Des. Dev.* **1,** 96 (1962).
3. Carter, J. L., Cusumano, J. A., and Sinfelt, J. H., *J. Phys. Chem.* **70,** 2257 (1966).
4. Van Hardeveld, R., and Van Montfoort, A., *Surf. Sci.* **4,** 396 (1966).
5. Bartholomew, C. H., Pannell, R. B., and Fowler, R. W., *Prepr. Div. Pet. Chem. Amer. Chem. Soc.* **22**(4), 1331 (August 1977).
6. Richardson, J. T., and Crump, J. G., *J. Catal.* **57,** 417 (1979).
7. Desai, P., and Richardson, J. T., *in* "Catalyst Deactivation" (B. Delmon and G. F. Froment, Eds.), p. 149. Elsevier, Amsterdam, 1980.
8. Kuo, H. K., Ganesan, P., and De Angelis, R. J., *J. Catal.* **64,** 303 (1980).

9. Bartholomew, C. H., and Farrauto, R. J., *J. Catal.* **45,** 41 (1976).
10. Bartholomew, C. H., "Alloy Catalysts with Monolith Supports for Methanation of Coal-Derived Gases." Final Report submitted to ERDA, FE-1790-9, September 6, 1977.
11. Pannell, R. B., Chung, K. S., and Bartholomew, C. H., *J. Catal.* **46,** 340 (1977).
12. Bartholomew, C. H., and Pannell, R. B., *J. Catal.* **65,** 390 (1980).
13. Klug, H. P., and Alexander, L. E., "X-Ray Diffraction Procedures for Polycrystalline and Amorphous Materials." Wiley, New York, 1954.
14. Mustard, D. G., and Bartholomew, C. H., *J. Catal.* **67,** 186 (1981).
15. Sorensen, W. L., and Bartholomew, C. H., *J. Catal.*, in press.
16. Wanke, S. E., and Flynn, P. C., *Catal. Rev.* **12,** 93 (1975).
17. Anderson, J. R., "Structure of Metallic Catalysts," pp. 46–54. Academic Press, New York, 1975.
18. Brenner, A., and Burwell, R. L., Jr., *J. Catal.* **52,** 353 (1978).
19. Boudart, M., *in* "Advances in Catalysis and Related Subjects," Vol. 20, p. 153. Academic Press, New York, 1969.
20. Bartholomew, C. H., Pannell, R. B., and Butler, J. L., *J. Catal.* **65,** 335 (1980).
21. Kelley, R. D., Goodman, D. W., and Madey, T. E., *Prepr. Div. Fuel Chem. Amer. Chem. Soc.* **25**(2), 43 (1980).
22. Vannice, M. A., *J. Catal.* **37,** 449 (1975).